

Confinement in the Deconfined Phase: A numerical study with a cluster algorithm *

K. Holland

Center for Theoretical Physics,
Laboratory for Nuclear Science, and Department of Physics
Massachusetts Institute of Technology (MIT)
Cambridge, Massachusetts 02139, U.S.A.

`holland@ctp.mit.edu`

MIT Preprint, CTP 2832

October 18, 2018

Abstract

We have previously found analytically a very unusual and unexpected form of confinement in $SU(3)$ Yang-Mills theory. This confinement occurs in the deconfined phase of the theory. The free energy of a single static test quark diverges, even though it is contained in deconfined bulk phase and there is no QCD string present. This phenomenon occurs in cylindrical volumes with a certain choice of spatial boundary conditions. We examine numerically an effective model for the Yang-Mills theory and, using a cluster algorithm, we observe this unusual confinement. We also find a new way to determine the interface tension of domain walls separating distinct bulk phases.

*This work is supported in part by funds provided by the U.S. Department of Energy (D.O.E.) under cooperative research agreement DE-FC02-94ER40818.

1 Introduction

In this paper, we investigate numerically an analytical result discussed in a previous paper [1], where we derived the finite volume dependence of the Polyakov loop in cylinders with particular boundary conditions. The analytical result tells us that, even in the deconfined phase, an external static quark is still confined. Confinement of quarks is usually described by a string tension σ , which is the energy cost per unit length of the QCD string connecting the fundamental charges. This unusual confinement is due to the multiple degenerate deconfined phases and has an effective “string tension” σ' , which depends on the energy cost of a domain wall separating two deconfined phases. In this paper, we observe numerically this unusual confinement in an effective model for the Yang-Mills theory. Using a cluster algorithm, we can accurately determine the energy cost of these domain walls. In addition, we derive a new analytical result for the finite volume behavior of the Polyakov loop near the deconfinement phase transition, which we also examine numerically with a cluster algorithm. In Section 2, we present the analytical calculations, in Section 3, we give the details of the numerical work and in Section 4, we briefly draw our conclusions.

2 Analytical dilute interface gas calculations

$SU(3)$ Yang-Mills theory at non-zero temperature lives in four-dimensional Euclidean space-time, with gauge fields $A_\mu(\vec{x}, t) = ieA_\mu^a(\vec{x}, t)\lambda^a$. The non-zero temperature is $T = 1/\beta$, where β is the extent in the periodic time direction, i.e. $A_\mu(\vec{x}, t + \beta) = A_\mu(\vec{x}, t)$. The action $S[A_\mu] = \int_0^\beta dt \int d^3x (1/2e^2) \text{Tr} F_{\mu\nu} F_{\mu\nu}$, is constructed from the field strength $F_{\mu\nu} = \partial_\mu A_\nu - \partial_\nu A_\mu + [A_\mu, A_\nu]$. The action is invariant under gauge transformations $A'_\mu = g^\dagger(A_\mu + \partial_\mu)g$, where the $SU(3)$ matrices $g(\vec{x}, t)$ are also periodic in the time direction. From our point of view, the most important field in the theory is the Polyakov loop,

$$\Phi(\vec{x}) = \text{Tr}[\mathcal{P} \exp \int_0^\beta dt A_4(\vec{x}, t)], \quad (1)$$

which is complex-valued and is built from the Euclidean time component of the gauge field. The Polyakov loop measures the response of the gauge field to the presence of a static test quark. Quantitatively, the free energy F of the test quark is given by the expectation value $\langle \Phi \rangle = \exp(-\beta F)$. If the quark is confined, then F diverges and $\langle \Phi \rangle = 0$, while if the quark is deconfined, F is finite and $\langle \Phi \rangle \neq 0$. The Polyakov loop transforms non-trivially under a global symmetry of the action S . If the gauge transformations are not quite periodic in the time direction, but are instead twisted, i.e.

$$g(\vec{x}, t + \beta) = g(\vec{x}, t)z, \quad z \in \mathbf{Z}(3) = \{\exp(2\pi in/3), n = 1, 2, 3\}, \quad (2)$$

the action is invariant but the Polyakov loop changes into $\Phi'(\vec{x}) = \Phi(\vec{x})z$. If $\langle\Phi\rangle = 0$, then the Polyakov loop value does not break this global symmetry — zero times z is still zero. However, if $\langle\Phi\rangle \neq 0$, this global symmetry is spontaneously broken. The Polyakov loop is the order parameter for this global symmetry — the $\mathbf{Z}(3)$ center symmetry. If the symmetry is intact, the quark is confined; if it is broken, the quark is deconfined. In fact, we know that the symmetry is spontaneously broken at high temperatures [2].

We study finite volumes to see whether or not the global symmetry is spontaneously broken in the infinite volume limit. In finite volumes, the system is sensitive to the spatial boundary conditions. For example, we could choose all spatial directions to obey periodic boundary conditions. However, $\langle\Phi\rangle$ would then always be zero, independent of temperature. This is because the Polyakov loop represents a static charge and Gauss' law implies that one can't have a charge contained in a torus [3]. We instead apply periodic boundary conditions in only two spatial directions, call them x and y . In the third direction z we use what are called charge conjugate or C -periodic boundary conditions [4]. If a field is C -periodic, it is replaced by its charge conjugate when translated by one period. For example, C -periodicity for gauge fields with period L_z means that

$$A_\mu(\vec{x} + L_z\vec{e}_z, t) = A_\mu(\vec{x}, t)^*, \quad (3)$$

where $*$ denotes complex conjugation. Being constructed from the gauge field, the Polyakov loop satisfies C -periodicity in the z -direction and we ask that the gauge transformations also satisfy this boundary condition. Note that charge conjugation is a symmetry of the Yang-Mills action. It is a useful boundary condition to apply because the center electric flux coming out of a quark can escape and end on the partner anti-quark on the other side of the C -periodic boundary. Now we can have a single charge in a finite volume. However, C -periodicity does break the $\mathbf{Z}(3)$ center symmetry [5], as we see from

$$g(\vec{x}, t)^* = g(\vec{x}, t + \beta)^* z = g(\vec{x} + L_z\vec{e}_z, t + \beta) z = g(\vec{x} + L_z\vec{e}_z, t) z^2 = g(\vec{x}, t)^* z^2. \quad (4)$$

This forces $z^2 = 1$ and as $z \in \mathbf{Z}(3)$, therefore $z = 1$. This means that we no longer have the freedom to twist the gauge transformations. This explicit breaking of the $\mathbf{Z}(3)$ center symmetry vanishes in the infinite volume limit. In a finite volume, $\langle\Phi\rangle$ is always non-zero. If the quark is confined, then $\langle\Phi\rangle$ vanishes in the infinite volume limit. Alternatively, if the quark is deconfined, $\langle\Phi\rangle$ remains non-zero, if the infinite volume limit is taken in cubic volumes.

We examine analytically how the Polyakov loop behaves in finite cylindrical volumes of dimension $L_x \times L_y \times L_z$, where $L_z \gg L_x, L_y$. We impose ordinary periodicity in the x - and y -directions and C -periodicity in the z -direction. First, we consider the system at low temperature, where quarks are confined. We view the partition function of the system diagrammatically as

$$Z = \boxed{c} = \exp(-\beta f_c A L_z), \quad (5)$$

where $A = L_x L_y$ is the cross-sectional area of the cylinder and f_c is the temperature-dependent bulk free energy density of the confined phase. The partition function is the sum of the Boltzmann weights over all possible configurations of the system. At low temperature, the entire volume is filled with bulk confined phase. We obtain $\langle \Phi \rangle$ diagrammatically from

$$Z\langle \Phi \rangle = \boxed{\text{---} c \text{---}} = \exp(-\beta f_c A L_z) \Sigma_0 \exp(-\beta \sigma L_z). \quad (6)$$

Because the Polyakov loop represents a static test quark and the quark is in confined bulk phase, there is a QCD string carrying the color flux from the quark to its partner anti-quark a distance L_z away on the other side of the C -periodic boundary. The line in the diagram represents the QCD string, with its string tension σ . Knowing $\langle \Phi \rangle = \Sigma_0 \exp(-\beta \sigma L_z)$, we find the free energy of the quark is $F = -1/\beta \ln \Sigma_0 + \sigma L_z$. This diverges as $L_z \rightarrow \infty$, i.e. as the quark and anti-quark are pulled infinitely far apart — the quark is indeed confined.

It has been shown that $SU(3)$ Yang-Mills theory has a first order phase transition at a temperature T_c [6]. Below T_c , external static quarks are confined. Above T_c , quarks are deconfined. Deconfinement is signalled by a non-zero value for $\langle \Phi \rangle$ which breaks the global $\mathbf{Z}(3)$ center symmetry. In the deconfined bulk phase, $\langle \Phi \rangle$ can take any one of three values,

$$\Phi^{(1)} = (\Phi_0, 0), \quad \Phi^{(2)} = \left(-\frac{1}{2}\Phi_0, \frac{\sqrt{3}}{2}\Phi_0\right), \quad \Phi^{(3)} = \left(-\frac{1}{2}\Phi_0, -\frac{\sqrt{3}}{2}\Phi_0\right). \quad (7)$$

Each value represents a distinct phase that the system can fall into and these phases can be rotated into one another by an element of $\mathbf{Z}(3)$. Above T_c , the center symmetry is broken, giving us three distinct degenerate deconfined bulk phases. Because there is more than one phase, different parts of the cylinder can be in different deconfined phases. In a cylinder, the phases tend to be separated by interfaces which are transverse to the long direction. The phases on either side of an interface are labelled by their value of $\langle \Phi \rangle$, d_i means deconfined phase with the expectation value $\langle \Phi \rangle = \Phi^{(i)}$. An interface between two different deconfined phases has a temperature-dependent interface tension, which is the energy cost per unit area $\alpha_{dd} = F/A$. Our diagrammatic expansion of the partition function corresponds to summing the Boltzmann weights over all configurations with all possible numbers of interfaces, assuming a dilute gas of interfaces [7]. The diagrammatic expansion of the partition function is

$$Z = \boxed{d_1} + \boxed{d_2} \boxed{d_3} + \boxed{d_3} \boxed{d_2} + \dots \quad (8)$$

C -periodicity in the z -direction means that certain configurations are not possible, for example, the volume with no interfaces cannot be entirely filled with either deconfined phase d_2 or d_3 . The terms corresponding to the diagrams are

$$\begin{aligned}
Z &= \exp(-\beta f_d A L_z) \\
&+ 2 \int_0^{L_z} dz \exp(-\beta f_d A z) \gamma \exp(-\beta \alpha_{dd} A) \exp(-\beta f_d A (L_z - z)) + \dots \\
&= \exp(-\beta f_d A L_z) [1 + 2\gamma \exp(-\beta \alpha_{dd} A) L_z + \dots].
\end{aligned} \tag{9}$$

As well as including a Boltzmann weight for the energy cost of the deconfined phase with free energy density f_d , we must also include the additional energy cost of an interface. The factor γ is included because the interfaces are not rigid and actually fluctuate. It has been shown that, in three dimensions, γ is to leading order independent of the area A [8]. To sum over all possible configurations, we integrate over all possible positions of the interfaces. We sum the interface expansion to all orders and find

$$Z = \exp(-\beta f_d A L_z + 2\gamma \exp(-\beta \alpha_{dd} A) L_z). \tag{10}$$

To calculate $\langle \Phi \rangle$, we again sum over all possible configurations. With the Boltzmann weight of each possible configuration, we also include the value of the Polyakov loop for that configuration. This gives the expansion

$$\begin{aligned}
Z \langle \Phi \rangle &= \exp(-\beta f_d A L_z) \left\{ \Phi^{(1)} + \int_0^{L_z} dz \gamma \exp(-\beta \alpha_{dd} A) \right. \\
&\times \frac{1}{L_z} [\Phi^{(2)} z + \Phi^{(3)} (L_z - z) + \Phi^{(3)} z + \Phi^{(2)} (L_z - z)] + \dots \left. \right\} \\
&= \Phi_0 \exp(-\beta f_d A L_z) \{1 - \gamma \exp(-\beta \alpha_{dd} A) L_z + \dots\} \\
&= \Phi_0 \exp(-\beta f_d A L_z - \gamma \exp(-\beta \alpha_{dd} A) L_z),
\end{aligned} \tag{11}$$

where, in the final line, we have summed the expansion to all orders. Dividing out the partition function, this gives us the result that

$$\langle \Phi \rangle = \Phi_0 \exp(-3\gamma \exp(-\beta \alpha_{dd} A) L_z). \tag{12}$$

This is an unusual result — it means that the free energy of a static quark is $F = (-1/\beta) \ln \Phi_0 + (3\gamma/\beta) \exp(-\beta \alpha_{dd} A) L_z$. If A is held fixed, this diverges as $L_z \rightarrow \infty$. As the quark and anti-quark are pulled infinitely far apart, the free energy cost becomes infinite. The quark is confined, even though there is no QCD string and we only have deconfined phases present. The confinement is due to the multiple degenerate deconfined phases lining up along the cylinder in definite domains, which are separated by domain walls. We would not see this effect if we had considered a cubic volume, as it would have been entirely filled with deconfined phase d_1 . Also, if we had chosen all spatial directions to be C -periodic, the volume would again only contain phase d_1 . The free energy F would then be independent of the volume, as we would expect in the deconfined phase. This unexpected confinement has an effective “string tension” $\sigma' = (3\gamma/\beta) \exp(-\beta \alpha_{dd} A)$ which is area and temperature dependent. We will observe this unusual confinement numerically and will also use the dependence of σ' on the area of the cylinder to extract the interface tension α_{dd} .

We now derive a new analytical result for the finite volume dependence of the Polyakov loop near the phase transition. Because the phase transition is of first order, as we approach the critical temperature T_c from above, the three deconfined phases can coexist with the single confined phase. We now implement a different choice of spatial boundary conditions. We impose C -periodicity in all spatial directions. This means that the complex deconfined phases d_2 and d_3 do not appear in the cylinder. With these new spatial boundary conditions, the diagrammatic expansion for the partition function near criticality is

$$\begin{aligned}
Z = & \boxed{c} + \boxed{d_1} \\
& + \boxed{c} \boxed{d_1} \boxed{c} + \boxed{d_1} \boxed{c} \boxed{d_1} + \dots
\end{aligned} \tag{13}$$

There are now only interfaces between confined and deconfined phases, which have an interface tension α_{cd} and a factor δ which includes the fluctuations of these domain walls. We sum the Boltzmann weights for all possible configurations to obtain

$$Z = 2 \exp(-\beta(f_c + f_d)AL_z/2) \cosh(L_z \sqrt{x^2 + \delta'^2}). \tag{14}$$

The quantity $x = \beta(f_c - f_d)A/2$ measures how far away we are from the finite volume critical point (where $f_c = f_d$) and $\delta' = \delta \exp(-\beta\alpha_{cd}A)$. To calculate $Z\langle\Phi\rangle$, as before, we include the value of the Polyakov loop with the Boltzmann weight for each possible configuration. With C -periodicity in all spatial directions, the static test quark has a neighboring anti-quark in all directions. If the test quark is placed in a region of confined bulk phase, a QCD string connects the quark to the nearest anti-quark, which will be in the x - or y -direction. Including the additional energy cost of the QCD string, we calculate

$$\begin{aligned}
\langle\Phi\rangle = & \left\{ \left[\frac{\Phi_0 + \Sigma'_0}{2} + \frac{x(\Phi_0 - \Sigma'_0)}{2\sqrt{x^2 + \delta'^2}} \right] \exp(L_z \sqrt{x^2 + \delta'^2}) + \right. \\
& \left. \left[\frac{\Phi_0 + \Sigma'_0}{2} - \frac{x(\Phi_0 - \Sigma'_0)}{2\sqrt{x^2 + \delta'^2}} \right] \exp(-L_z \sqrt{x^2 + \delta'^2}) \right\} / 2 \cosh(L_z \sqrt{x^2 + \delta'^2}),
\end{aligned} \tag{15}$$

where $\Sigma'_0 = \Sigma_0 \exp(-\beta\sigma L_\perp)$, $L_\perp = \min(L_x, L_y)$. We test this new result in two limits. If we are on the deconfined side of the phase transition, then $f_d < f_c$ and we find that, as the volume grows large, $\langle\Phi\rangle = \Phi_0$. This is as we expect — a domain wall costs more and more energy, so the whole volume is filled with deconfined phase d_1 and the quark energy is independent of the volume size. If we are on the confined side of the phase transition with $f_d > f_c$, as the volume becomes large, $\langle\Phi\rangle = \Sigma_0 \exp(-\beta\sigma L_\perp)$ and $F = (-1/\beta) \ln \Sigma_0 + \sigma L_\perp$. The entire volume is filled with confined phase and the quark is connected to the nearest anti-quark by a QCD string. This analytical result shows how the finite volume behavior of the Polyakov loop changes across the deconfinement phase transition with C -periodicity in all directions. We also use this expression to extract the confined-deconfined interface tension α_{cd} .

3 Numerical investigation of the Potts Model

From the analytical calculations for $SU(3)$ Yang-Mills theory, we expect to see unusual confinement even deep in the deconfined phase. If we can observe such behavior numerically, we can extract properties of domain walls, such as the deconfined-deconfined interface tension α_{dd} . The analytical calculation assumes that there are definite deconfined domains which line up along the cylinder separated by interfaces. While this is certainly true if the volume is arbitrarily large, it is not at all clear if this phenomenon can be observed in moderately sized volumes. The Polyakov loop expectation value should become exponentially small as the cylinder length grows. It will certainly be very difficult to detect numerically such a small signal for Yang-Mills theory. We want to know if this volume dependence is at all observable. We will examine the 3-d 3-state Potts model, which is an effective model for non-zero temperature $SU(3)$ Yang-Mills theory. We will explain why it is an effective model and show how we can observe the unusual confinement even in relatively small volumes using highly efficient numerical techniques.

In the 3-d 3-state Potts model, there are spins Φ_x at positions x which can take one of three values $\Phi_x \in \mathbf{Z}(3) = \{\exp(2\pi in/3), n = 1, 2, 3\}$. The action is

$$S[\Phi] = -\beta \sum_{\langle xy \rangle} \delta_{\Phi_x, \Phi_y}, \quad (1)$$

where the sum is over nearest neighbors. If we globally rotate all spins by $\Phi'_x = \Phi_x z, z \in \mathbf{Z}(3)$, the action is unchanged. This global symmetry is exactly analogous to the $\mathbf{Z}(3)$ center symmetry of the Yang-Mills theory. Numerical work shows that this model has a first order phase transition at a non-zero temperature T_c [12]. For $T > T_c$, the system is in a disordered phase, where $\langle \Phi \rangle$ is zero and the global $\mathbf{Z}(3)$ symmetry is intact. For $T < T_c$, there are three ordered phases, where $\langle \Phi \rangle \propto \exp(2\pi in/3), n = 1, 2, 3$ and the global $\mathbf{Z}(3)$ symmetry is broken. The disordered phase is exactly analogous to the confined phase of the Yang-Mills theory, while the three ordered phases correspond to the three deconfined phases. Because of this shared global symmetry and phase structure, the Potts model is an effective theory to describe the deconfinement phase transition. We look at the behavior of Potts spins in cylindrical volumes which are periodic in x and y and C -periodic in z . We can again apply C -periodicity in the z -direction because charge conjugation is a symmetry of the Potts action. Using the dilute gas of interfaces, we calculate that the average spin $\langle \Phi \rangle$ in this volume deep in the ordered (deconfined) regime is

$$\langle \Phi \rangle = \Phi_0 \exp(-3\gamma \exp(-\beta\alpha_{dd}A)L_z). \quad (2)$$

Now we have an interface tension α_{dd} for an interface between two ordered phases and γ accounts for the fluctuation of these non-rigid domain walls. Previously, the Polyakov loop fell off exponentially with the cylinder length, signalling confinement. This now becomes the exponential fall off of the average spin. Similarly, we calculate

the average spin near the phase transition applying C -periodicity in all spatial directions and we see that this depends on α_{cd} , the energy cost of an interface between an ordered and a disordered phase. The analytical results are identical, translating deconfined and confined bulk phases into ordered and disordered bulk phases.

We measure the average spin $\langle \Phi \rangle$ using a cluster algorithm [13]. We pick a spin at random from the cylinder as the first element of a cluster. Next, we examine all nearest neighbors of this spin. If a neighbor has the same spin value, we include it in the cluster with probability $P = 1 - \exp(-\beta)$. If a neighboring spin has a different value, we do not include it — all the spins in a cluster have the same value. We continue to build a cluster until all neighbors of all spins in the cluster have been examined. In a multi-cluster algorithm, we keep building clusters until the entire volume is decomposed into many clusters. Once all the clusters are built, all the spins in each cluster are flipped to a new value. However, it is not always possible to flip a cluster. If a cluster winds around a C -periodic direction of the cylinder an odd number of times, it must contain spins with real value 1. Otherwise, it would not satisfy C -periodicity in this direction. The spins in such a cluster cannot be flipped to a new complex value as this would break the C -periodicity. Such a cluster is called a wrapping cluster. Any other type of cluster is called non-wrapping and can always be flipped. In a multi-cluster algorithm, the average spin is

$$\langle \Phi \rangle = \frac{1}{N_V} \langle \sum_x \Phi_x \rangle = \frac{1}{N_V} \langle \sum_C \sum_{x \in C} \Phi_x \rangle = \frac{1}{N_V} \langle \sum_C N_C \langle \Phi \rangle_C \rangle, \quad (3)$$

i.e. the average spin is the average over all spins in the volume divided by the total number of spins N_V . We can sum all the spins in two steps — first we sum over all the spins contained in a single cluster C , then we sum over all the clusters. Allowing the spins in each cluster to flip to all possible states, we sum the average spin in each cluster $\langle \Phi \rangle_C$ times the number of spins in each cluster N_C . What is the average spin in a cluster? In a wrapping cluster, the spins must always have real value 1 and so these clusters have $\langle \Phi \rangle_C = 1$. The spins in a non-wrapping cluster can take on all possible values and these clusters have $\langle \Phi \rangle_C = 0$. The entire volume is decomposed into clusters, the number of spins contained in the wrapping clusters is counted and the clusters are flipped to new values. This is repeated sufficiently often to numerically estimate the average number of spins contained in wrapping clusters. This is an improved estimator because we only add non-negative numbers in our estimate of $\langle \Phi \rangle$. We can also use a single cluster algorithm. Instead of calculating the average spin by summing the average spin of all clusters, we only determine the average spin in one single cluster C . The probability of choosing this cluster from all of them is proportional to its size, i.e. $P_C = N_C/N_V$. The average spin is then

$$\langle \Phi \rangle = \langle \frac{N_C}{N_V} \frac{\langle \Phi \rangle_C}{P_C} \rangle = \langle \langle \Phi \rangle_C \rangle = P_{\text{wrap}}, \quad (4)$$

the sum over all cluster averages is replaced by one cluster average divided by the probability P_C of choosing that cluster. The average spin in the entire volume equals

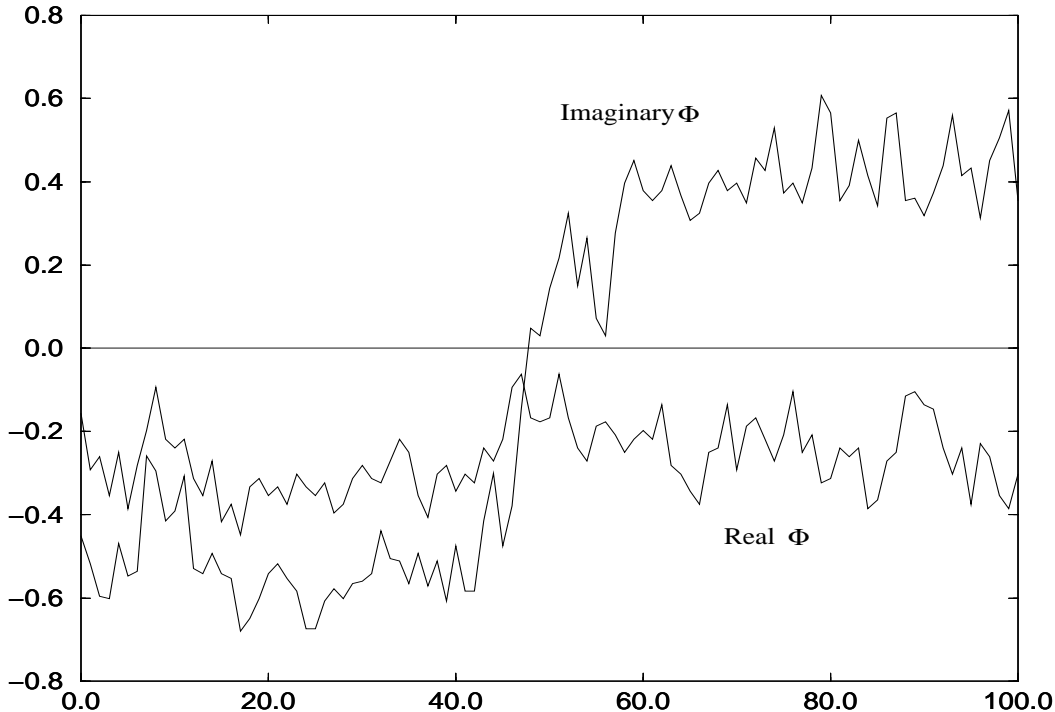


Figure 1: *The spins Φ_x are averaged over the transverse plane located at longitudinal coordinate z . The plot is of the real and imaginary parts of the planar average of the spin versus z . There is one interface, separating two of the ordered bulk phases.*

the average spin in the single cluster that we build, which equals the probability P_{wrap} that the single cluster is a wrapping cluster. To estimate this probability numerically, we build a single cluster; if it is wrapping, we count a 1, if it is non-wrapping, we count a 0. We repeat this procedure until we can accurately estimate the wrapping probability. Again, this is an improved estimator because we only add non-negative numbers in making our estimate of P_{wrap} . For very long and thin cylinders, P_{wrap} is very small and such a small signal would be very difficult to detect if we had positive and negative contributions to our estimator with lots of cancellation. The signal is small but the improved estimator does the best possible job of numerically estimating the probability. A previous study of the Ising model has used an algorithm where boundary conditions can be changed depending on the properties of clusters [14].

We first consider the case deep in the ordered phase of the theory, where we expect $\langle \Phi \rangle$ to decrease exponentially with the cylinder length, which is the signal in this effective model for the unusual confinement. Here, we use the single cluster algorithm to estimate $\langle \Phi \rangle$. Previous work has determined that the phase transition occurs at $\beta_c = 0.550565(10)$ [12]. The ordered regime is $\beta > \beta_c$. If we go too far away from β_c , the energy cost of even one interface will be very large, an interface will practically never appear in the volume and our analytical calculation will not apply. We work in a region $\beta_c < \beta < 1.005\beta_c$, where typically there are interfaces in the

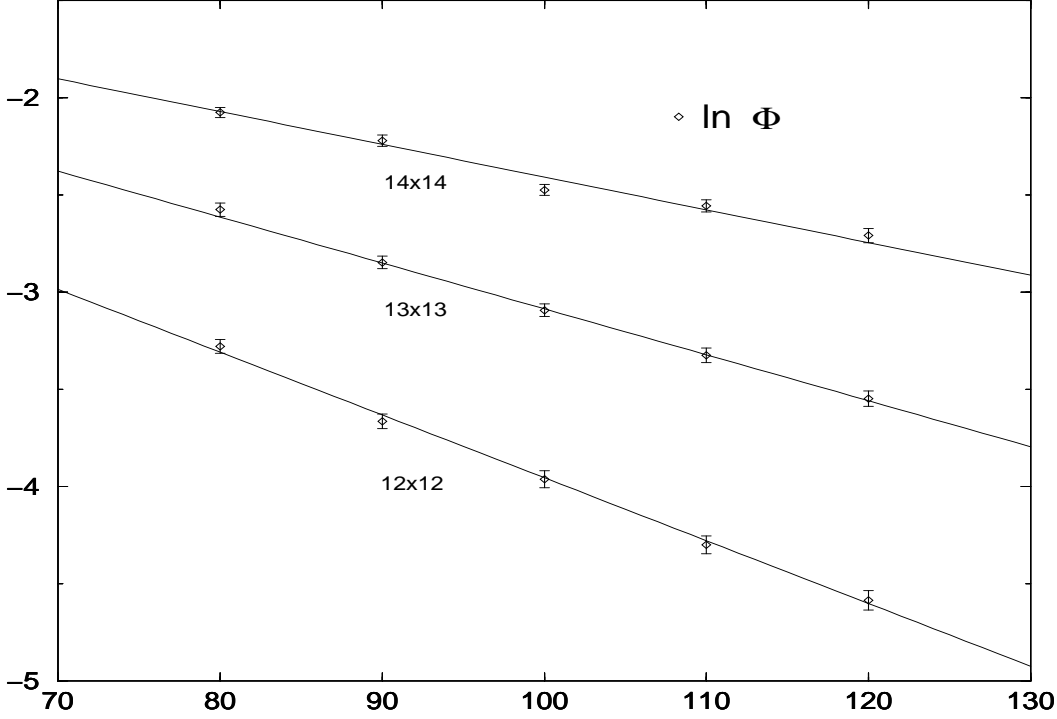


Figure 2: A plot of $\ln\langle\Phi\rangle$ versus L_z , the cylinder length. The lines are the fit to the analytical calculation of $\ln\langle\Phi\rangle$ in the ordered phase regime.

cylinder. The volumes we examine are of transverse dimension $L_x = L_y = 12, 13, 14$ and L_z in the range 80 to 120. In Figure 1, we show a typical numerical configuration of a volume of dimension $12 \times 12 \times 100$ at a temperature $\beta = 1.003\beta_c$. This particular configuration has one interface with bulk ordered phase $\Phi = (-1/2 - i\sqrt{3}/2)\Phi_0$ on the left hand side and ordered phase $\Phi = (-1/2 + i\sqrt{3}/2)\Phi_0$ on the right.

In Figure 2, we have plotted the numerical results for $\ln\langle\Phi\rangle$ in cylinders of various lengths and areas obtained at a particular temperature, here $\beta = 1.0035\beta_c$. We see clearly that the average spin falls off exponentially with the length of the cylinder. The single cluster algorithm and associated improved estimator are able to detect this extremely small signal. We see that our analytical calculation, which is certainly true for arbitrarily large volumes, also holds for volumes of moderate size. We fit the numerical data to the analytical formula and each line in Figure 2 corresponds to cylinders with a fixed area, i.e. $12 \times 12, 13 \times 13$ and 14×14 . All three lines are obtained from one fit, which gives the numerical value of $\alpha_{dd}(\beta)$ with χ^2 per degree of freedom ~ 0.7 . We take this to be an indication of a good fit. We have performed simulations at many values of β , including one previously examined in the literature, allowing us to make a direct comparison of the interface tension. At $\beta = 0.552$, a value of $\alpha_{dd} = 0.01796(14)$ has previously been determined [15]. Using our technique, we find $\alpha_{dd} = 0.01838(42)$, which is in agreement within error bars. In Figure 3, we have plotted the values we have determined for α_{dd} as a function of

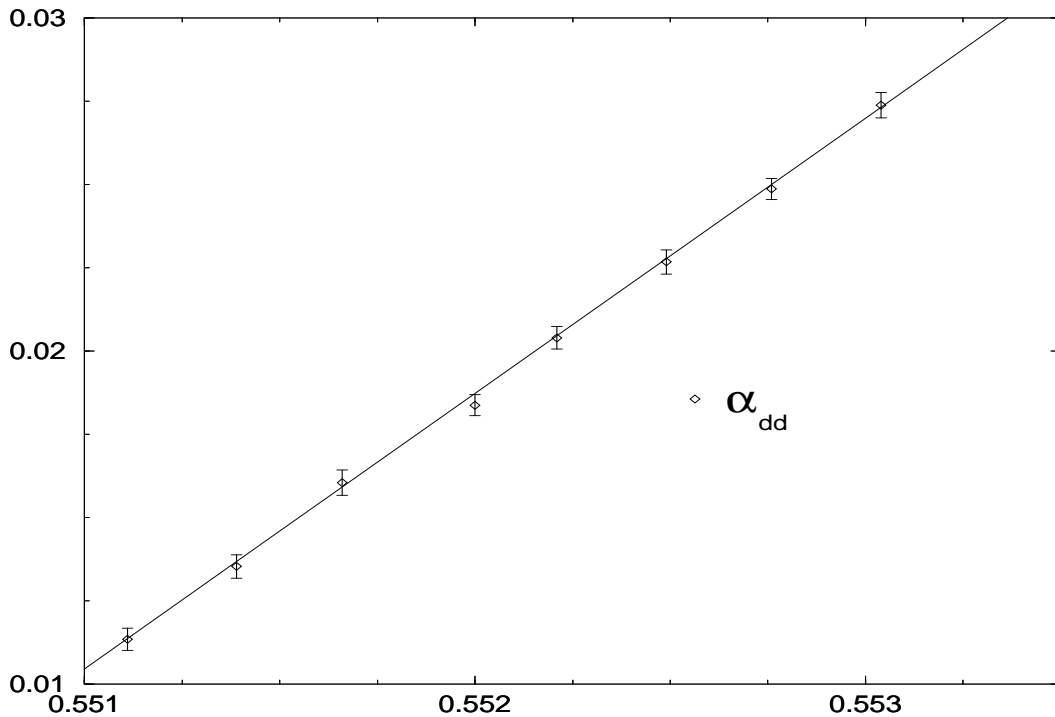


Figure 3: *The ordered-ordered interface tension α_{dd} as a function of β . The fit is a straight line.*

β . The data fits very well to a straight line, with $\chi^2/\text{d.o.f} \sim 0.2$. The fit is

$$\alpha_{dd}(\beta) = -4.54(4) + 8.26(8)\beta, \quad (5)$$

where the uncertainties in the final digits are paranthesized. The uncertainties appear rather large, but are actually highly correlated. At the critical point, it is expected that $\alpha_{dd}(\beta_c) = 2\alpha_{cd}$ due to a phenomenon called complete wetting. It is tempting to extrapolate our linear fit to the critical point to estimate α_{cd} . However, our configurations do not contain disordered phase and our numerical data cannot know anything about the energy cost of an ordered-disordered domain wall. We cannot extrapolate the fit deep in the ordered phase to the critical point.

We cannot use the single cluster algorithm to verify our new analytical calculation near the phase transition, where we use C -periodicity in all directions. Using the single cluster algorithm, $\langle \Phi \rangle$ is equal to P_{wrap} . With C -periodicity in all directions, the probability of building a wrapping cluster is much greater and so the numerical signal is much larger. However, a wrapping cluster cannot be flipped to a new state and the configuration is unchanged after this iteration. The more often we build a wrapping cluster, the longer it takes for configurations to become independent of one another. Thus, a larger signal also means larger autocorrelations. In this case, the single cluster algorithm gives much larger integrated autocorrelation times than with C -periodicity in the long direction only. This makes the algorithm inefficient and we cannot detect finite volume dependence in $\langle \Phi \rangle$. In this instance, the multicluster

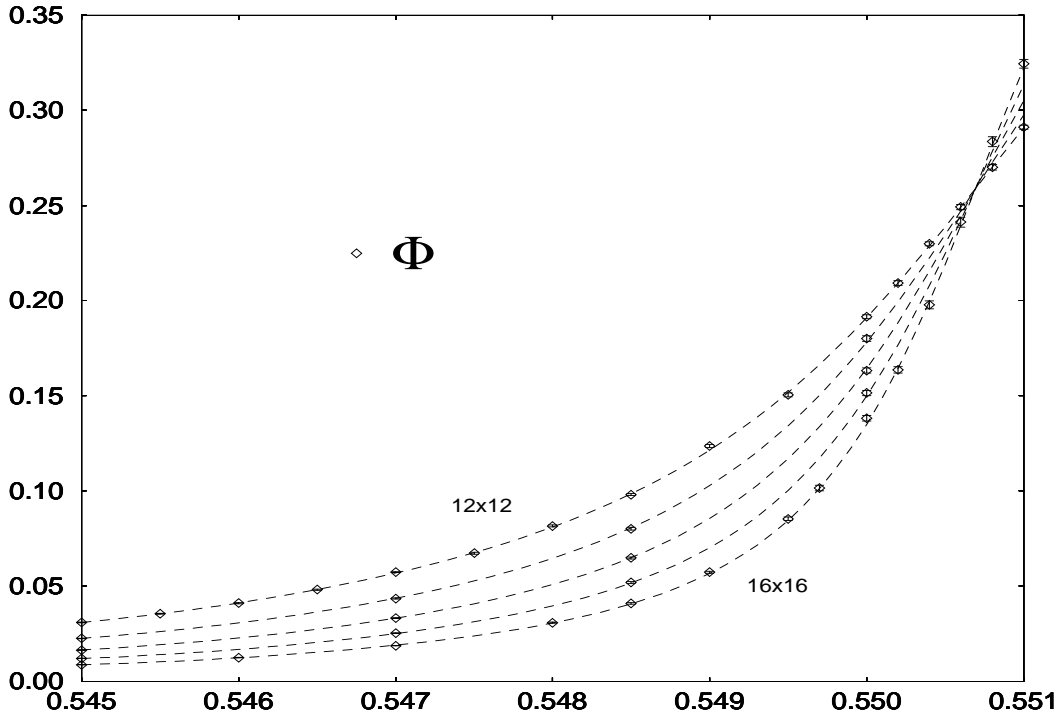


Figure 4: A plot of $\langle \Phi \rangle$ versus β in cylinders of length $L_z = 80$ and areas from 12×12 to 16×16 . The curves are the fit to the analytical behavior of $\langle \Phi \rangle$ across the phase transition.

algorithm is far superior. By decomposing the entire volume into clusters, there will always be many non-wrapping clusters which can be flipped and configurations very quickly become decorrelated. Using the multicluster algorithm, we examine cylinders with dimensions $L_x = L_y = 12, 13, 14, 15, 16$ and $L_z = 60, 70, 80, 90$ and at temperatures in the range $\beta \in [0.545, 0.551]$. We fit all of the data to the predicted analytical behavior of $\langle \Phi \rangle$. In Figure 4, we plot some of the numerical data and the fit of $\langle \Phi \rangle$ as a function of β . From the fit of all the data, we find the ordered-disordered interface tension is $\alpha_{cd} = 0.0015(2)$, with $\chi^2/\text{d.o.f} \sim 1.1$. Translated into our notation, a value of $\alpha_{cd} = 0.00148(2)$ has previously been found [12]. From the fit, we also obtain $\beta_c = 0.55070(17)$, in comparison to the previously quoted value $\beta_c = 0.550565(10)$ [12]. These values are consistent and we feel that the relatively large percentage errors in our estimates of the interface tension and the critical temperature may be because we work in smaller volumes. There are also other techniques to extract the interface tension near criticality [16].

4 Conclusions

Analytically, we predicted that a very unusual type of confinement occurs even in the deconfined phase of $SU(3)$ Yang-Mills theory. The free energy of a single static

quark diverges, even though it is contained in deconfined bulk phase. The signal for this unusual confinement is that the expectation value of the Polyakov loop becomes exponentially small. We have successfully observed this phenomenon numerically in an effective theory. It was not a priori clear that the exponentially small signal could be measured or that this confinement would be observable in moderately sized volumes. The single cluster algorithm and associated improved estimator can detect this very small signal in reasonably sized cylinders and accurately determine the energy cost of domain walls between distinct bulk phases. Our new analytical result predicts the finite volume behavior of the Polyakov loop across the deconfinement phase transition and we observe this behavior numerically, allowing us to estimate the energy cost of domain walls at criticality. Interestingly, this is an example where a multicluster algorithm is far superior to a single cluster algorithm.

5 Acknowledgements

I would like to acknowledge the essential contribution of U.-J. Wiese to this project.

References

- [1] K. Holland and U.-J. Wiese, Phys. Lett. B415 (1997) 179.
- [2] L. D. McLerran and B. Svetitsky, Phys. Rev. D24 (1981) 450.
- [3] E. Hilf and L. Polley, Phys. Lett. B131(1983) 412.
- [4] A. S. Kronfeld and U.-J. Wiese, Nucl. Phys. B357 (1991) 521.
- [5] U.-J. Wiese, Nucl. Phys. B375 (1992) 45.
- [6] R. V. Gavai, F. Karsch and B. Petersson, Nucl. Phys. B322 (1989) 738;
M. Fukugita, M. Okawa and U. Ukawa, Phys. Rev. Lett. 63 (1989) 1768;
N. A. Alves, B. A. Berg and S. Sanielevici, Phys. Rev. Lett. 64 (1990) 3107.
- [7] B. Grossmann, M. L. Laursen, T. Trappenberg and U.-J. Wiese, Nucl. Phys. B396 (1993) 584.
- [8] V. Privman and M. E. Fisher, J. Stat. Phys. 33 (1983) 385;
E. Brezin and J. Zinn-Justin, Nucl. Phys. B257 [FS14] (1985) 867.
- [9] Z. Frei and A. Patkós, Phys. Lett. B229 (1989) 102.
- [10] T. Trappenberg and U.-J. Wiese, Nucl. Phys. B372 (1992) 703.

- [11] K. Kajantie, L. Kärkkäinen and K. Rummukainen, Nucl. Phys. B333 (1990) 100; Nucl. Phys. B357 (1991) 693.
- [12] W. Janke and R. Villanova, Nucl. Phys. B489 [FS] (1997) 679, and references therein.
- [13] R. H. Swendsen and J. S. Wang, Phys. Rev. Lett. 58(1987) 86;
U. Wolff, Phys. Lett. B228 (1989) 379.
- [14] M. Caselle and M. Hasenbusch, Nucl. Phys. B470 (1996) 435.
- [15] M. Caselle, F. Gliozzi, P. Provero and S. Vinti, Nucl. Phys. Proc. Suppl. 34 (1994) 720.
- [16] M. Schmidt, Z. Phys. B95 (1994) 327;
J.-D. Wang and C. DeTar, Phys. Rev. D47 (1993) 4091;
B. A. Berg and T. Neuhaus, Phys. Rev. Lett. 68 (1992) 9;
B. Grossmann, M. L. Laursen, T. Trappenberg and U.-J. Wiese, Phys. Lett. B293 (1992) 175.